Original Article

MOLECULAR METABOLISM

The SSBP3 co-regulator is required for glucose homeostasis, pancreatic islet architecture, and beta-cell identity

Eliana Toren, Jessica D. Kepple, Kristen V. Coutinho, Samuel O. Poole, Iztiba M. Deeba, Tanya H. Pierre, Yanping Liu, Maigen M. Bethea, Chad S. Hunter*

ABSTRACT

Objective: Transcriptional complex activity drives the development and function of pancreatic islet cells to allow for proper glucose regulation. Prior studies from our lab and others highlighted that the LIM-homeodomain transcription factor (TF), Islet-1 (Isl1), and its interacting co-regulator, Ldb1, are vital effectors of developing and adult β-cells. We further found that a member of the Single Stranded DNA-Binding Protein (SSBP) co-regulator family, SSBP3, interacts with Isl1 and Ldb1 in β-cells and primary islets (mouse and human) to impact β-cell target genes *MafA* and *Glp1R in vitro*. Members of the SSBP family stabilize TF complexes by binding directly to Ldb1 and protecting the complex from ubiquitin-mediated turnover. In this study, we hypothesized that SSBP3 has critical roles in pancreatic islet cell function *in vivo*, similar to the Isl1::Ldb1 complex.

Methods: We first developed a novel *SSBP3* LoxP allele mouse line, where Cre-mediated recombination imparts a predicted early protein termination. We bred this mouse with constitutive Cre lines (*Pdx1*- and *Pax6*-driven) to recombine *SSBP3* in the developing pancreas and islet ($SSBP3^{\Delta Panc}$ and $SSBP3^{\Delta Islet}$), respectively. We assessed glucose tolerance and used immunofluorescence to detect changes in islet cell abundance and markers of β-cell identity and function. Using an inducible Cre system, we also deleted *SSBP3* in the adult β-cell, a model termed $SSBP3^{\Delta \beta\text{-}cell}$. We measured glucose tolerance as well as glucose-stimulated insulin secretion (GSIS), both *in vivo* and in isolated islets *in vitro*. Using islets from control and $SSBP3^{\Delta \beta\text{-}cell}$ we conducted RNA-Seq and compared our results to published datasets for similar β-cell specific *Ldb1* and *Isl1* knockouts to identify commonly regulated target genes.

Results: $SSBP3^{\Delta Panc}$ and $SSBP3^{\Delta Islet}$ neonates present with hyperglycemia. $SSBP3^{\Delta Islet}$ mice are glucose intolerant by P21 and exhibit a reduction of β-cell maturity markers MafA, Pdx1, and UCN3. We observe disruptions in islet cell architecture with an increase in glucagon$^+$ α-cells and ghrelin$^+$ ε-cells at P10. Inducible loss of β-cell SSBP3 in $SSBP3^{\Delta \beta\text{-}cell}$ causes hyperglycemia, glucose intolerance, and reduced GSIS. Transcriptomic analysis of 14-week-old $SSBP3^{\Delta \beta\text{-}cell}$ islets revealed a decrease in β-cell function gene expression (*Ins*, *MafA*, *Ucn3*), increased stress and dedifferentiation markers (*Neurogenin-3*, *Aldh1a3*, *Gastrin*), and shared differentially expressed genes between SSBP3, Ldb1, and Isl1 in adult β-cells.

Conclusions: SSBP3 drives proper islet identity and function, where its loss causes altered islet-cell abundance and glucose homeostasis. β-Cell SSBP3 is required for GSIS and glucose homeostasis, at least partially through shared regulation of Ldb1 and Isl1 target genes.

Keywords Diabetes; Glucose homeostasis; Pancreatic islet; Transcription factor; Co-regulator; Gene regulation

1. INTRODUCTION

Diabetes mellitus (DM) is an ever-growing global health crisis defined by glucose dysregulation, and in 2019 was the seventh leading cause of death in the United States [1]. Whether by autoimmune attack in Type 1 (T1D), or by insulin resistance and subsequent β-cell dysfunction in Type 2 (T2D), loss of functional insulin-producing β-cell mass is a central diabetes mechanism. To combat these pathophysiologies, β-cell rescue and replacement therapies have become a promising therapeutic avenue. Several groups are investigating the transplantation of stem-cell derived β-cells for diabetes patients, but models for reproducing β-cell development and functional maturation require optimization [2]. The advancement and implementation of these therapies hinges upon a comprehensive understanding of β-cell gene regulation [3]. The transcriptional complexes that govern β-cell development and function have the potential to provide instructions for their generation, repair, and survival.

Pancreatic islets are clusters of hormone-producing cells comprised of α, β, δ, ε, and pancreatic polypeptide (PP) cells that exist in varied abundances depending on the organism [4]. In mice, β-cells

Comprehensive Diabetes Center and Department of Medicine, Division of Endocrinology, Diabetes, and Metabolism, University of Alabama at Birmingham, Birmingham, AL 35294, USA

*Corresponding author. 1825 University Boulevard, SHEL 1211, University of Alabama at Birmingham, Birmingham, AL 35294, USA. E-mail: huntercs@uab.edu (C.S. Hunter).

Received May 15, 2023 • Revision received July 24, 2023 • Accepted July 31, 2023 • Available online 1 August 2023

https://doi.org/10.1016/j.molmet.2023.101785

Abbreviations

ChIP	chromatin immunoprecipitation
Co-IP	co-immunoprecipitation
CRHR2	corticotropin releasing hormone receptor 2
DM	diabetes mellitus
DEG	differentially expressed gene
DD	dimerization domain
E	embryonic day
GTT	glucose tolerance test
GSIS	glucose-stimulated insulin secretion
HD	homeodomain
Isl1	Islet-1
LCCD	Ldb1/Chip Conserved Domain
LIM	Lin11-Isl1-Mec3
Ldb1	LIM domain binding protein 1
LIM-HD	LIM-Homeodomain
LID	LIM interaction domain
PP	pancreatic polypeptide
P	postnatal day
PCA	principal component analysis
SSBP	single-stranded DNA-binding protein
TF	transcription factor
T1D	type 1 diabetes
T2D	type 2 diabetes

are the most abundant (~80%) and exist in the islet core, and glucagon-producing α-cells (~10–15%) reside in the peripheral mantle with δ, ε, and PP cells. Postprandial β-cell-derived insulin stimulates glucose uptake to reduce blood glucose levels to protect from hyperglycemia [5]. α-Cell-derived glucagon acts primarily on the muscle and liver where it triggers glycogenolysis - the conversion of stored glycogen into glucose, which is then released into the blood stream to prevent hypoglycemia [6]. δ-Cells interact with both α- and β-cells and secrete the somatostatin hormone, which has local inhibitory effects on glucagon and insulin secretion [7]. The ghrelin-producing ε-cell remains understudied, but there is evidence for insulinostatic effects of ε-derived ghrelin that prevent insulin hypersecretion and hypoglycemia during fasting [8]. The coordinated functions of all five islet cell types are controlled by transcription factors (TFs) and while the β-cell is the most comprehensively studied, regulators of the other islet cell types are also key to understanding islet physiology and diabetes pathogenesis.

Islet-1 (Isl1) is a LIM (named for Lin11-Isl1-Mec3)-Homeodomain (HD) TF expressed in all hormone-producing cells of the adult islet, and is required for islet cell development and function [9–11]. Global Isl1 loss imparts embryonic lethality by embryonic day (E)10.5 due to requirements in cardiac mesoderm and central nervous system development [12,13]. To circumvent embryonic lethality, a pancreas-wide conditional *Isl1* knockout was created using *Pdx1-Cre*, resulting in drastically reduced islet hormones (insulin, glucagon, somatostatin) and subsequent progressive hyperglycemia and glucose intolerance [10]. Isl1 was shown to regulate the β-cell maturity marker gene *MafA* [10,14] and α-cell TF gene *Arx* [15], highlighting an islet-wide requirement for Isl1. Inducible loss of Isl1 in the adult β-cell caused glucose intolerance, and combined transcriptomic and cistromic analyses highlighted Isl1 regulation of *Insulin*, *MafA*, β-cell TF *Pdx1*, and *Slc2a2*, which encodes the β-cell glucose transporter GLUT2 [9,16].

While Isl1 has known β-cell roles, it has also been shown that Isl1 and other LIM-HD TFs act in large multimeric complexes [17]. The widely-expressed transcriptional co-regulator LIM-domain binding protein-1 (Ldb1) interacts with LIM-HD TFs, including Isl1, to impact transcription of diverse genes during development [18]. In the pancreas, our lab and others have shown that robust Ldb1::Isl1 interactions are required for islet-cell identity and function both during development and in the adult β-cell [16,19,20]. Ldb1 contains a dimerization (DD) and LIM-interaction domain (LID) allowing it to act as a dimerized scaffold for stabilizing large transcriptional complexes. To define novel Ldb1 or Isl1 interactions in the β-cell, we employed a reversible cross-link IP and mass spectrometry and observed enrichment of the single-stranded DNA-binding protein 3 co-regulator (SSBP3) [21].

The SSBP factors, including SSBP2-4, are a small family of Ldb1-interacting proteins. SSBPs have a conserved N-terminal FORWARD domain that interacts with the Ldb/Chip Conserved Domain (LCCD) of Ldb1, in addition to a proline-rich domain functionally linked to head development [17,22]. SSBP proteins govern LIM-complex activity by binding Ldb1 and protecting complexes from ubiquitin-mediated turnover by RLIM [23,24]. Coordinated activity of Isl1, Ldb1, and SSBP3 (formerly known as SSDP1 [22]) regulates head development [25], but prior to work from our group, SSBP3 activity in the pancreas was unexplored. In a 2015 study, we found that SSBP3 is expressed at high levels in β-cell lines, developing and adult mouse islets, and adult human islets [21]. siRNA-mediated knockdown in β-cell lines revealed that SSBP3 is required for expression of Ldb1 targets *MafA*, *Pdx1*, *Kcnj11*, and *Glp1R*. Co-immunoprecipitation (Co-IP) also highlighted that SSBP3::Ldb1 and SSBP3::Isl1 interactions are maintained in mouse and human islets, while chromatin immunoprecipitation (ChIP) in β-cell lines demonstrated SSBP3 occupancy of *MafA* and *Glp1R* regulatory domains. Through possible transcriptional coordination with Ldb1 and Isl1, we hypothesize that SSBP3 has critical *in vivo* regulatory roles in developing and adult islets and β-cells.

In this study, we generated a novel *SSBP3* LoxP mouse line to interrogate the *in vivo* role of SSBP3 in islet and β-cell function. We use *Pdx1-*, *Pax6-*, and inducible *MIP-Cre*^{ER} transgenic lines to create three temporal models of SSBP3 loss in the developing pancreas, islet, and adult β-cell, respectively. We found that mice lacking SSBP3 in the islet (*SSBP3*$^{\Delta Islet}$) are progressively hyperglycemic and glucose intolerant, similar to Isl1 and Ldb1 knockout models. We observed islet architecture defects in *SSBP3*$^{\Delta Islet}$ pancreata, an increase in glucagon^{+} and other non-β islet cells (including ghrelin), and a loss of β-cell maturity and functionality markers MafA, Glut2, and UCN3. Inducible adult β-cell SSBP3 loss (*SSBP3*$^{\Delta \beta\text{-cell}}$) also led to hyperglycemia, glucose intolerance, glucose-stimulated insulin secretion (GSIS) defects, and reductions of β-cell identity markers MafA, Pdx1, UCN3, and Glut2. Transcriptomic analysis of *SSBP3*$^{\Delta \beta\text{-cell}}$ islets revealed decreased β-cell function genes (*Ins1/2*, *MafA*, *UCN3*) and increased dedifferentiation markers (*Neurogenin-3*, *Aldh1a3*). We identified both expected (*MafA*) and novel (*Rfx6*, *Gastrin*) gene targets shared between SSBP3-, Isl1-, and Ldb1-deficiency models that provide valuable insight into shared β-cell regulatory networks. These findings firmly establish SSBP3 as a critical component of islet LIM-transcriptional

complexes and provide candidate targets for a deeper understanding of these complexes and their mechanisms.

2. MATERIALS AND METHODS

2.1. Generation of mouse lines

We designed a novel *SSBP3* LoxP (floxed) mouse line generated by the Jackson Laboratory using Crispr-Cas9 gene editing. Exon 4 of the 18-exon *SSBP3* gene is LoxP flanked, which partially encodes the Ldb1-interacting FORWARD domain (LoxP site details in Supplemental Figure 1). A schematic of the knockout strategy can be found in Figure 1A. $SSBP3^{F/F}$ females were crossed with $SSBP3^{F/+}$; Cre^{+} males to generate the three mouse models, as well as littermate controls (CTL) and heterozygotes ($SSBP3^{F/+}$; Cre^{+}). The $SSBP3^{\Delta Panc}$, $SSBP3^{\Delta Islet}$, and $SSBP3^{\Delta\beta\text{-}cell}$ models were generated using *Pdx1*- [26], *Pax6*- [27], and *MIP-Cre*^{ER} [28] males, respectively. $SSBP3^{\Delta Panc}$ mice were collected at postnatal day (P)1. For some $SSBP3^{\Delta Islet}$ studies, embryos were collected at E18.5, where the morning of vaginal plug detection was considered E0.5. Remaining data was collected from P1, P10, P21, P28, or P35. Both males and females were used for these studies. $SSBP3^{\Delta\beta\text{-}cell}$ induction began at four weeks of age, where 150 μg/g body weight of tamoxifen (Sigma—Aldrich, #T5648) was administered by oral gavage every other day for two weeks, as previously described [16]. $SSBP3^{\Delta\beta\text{-}cell}$ data were collected at 6-, 8-, 10-, 12-, and 14-weeks. Only males were used for $SSBP3^{\Delta\beta\text{-}cell}$ experiments, as females did not exhibit a glucose homeostasis phenotype unique from controls (Supplemental Figure 2A). We also generated *MIP-Cre*^{ER} CTLs to confirm there were no significant differences associated with Cre expression (Supplemental Figure 2B—C). All studies were approved by and performed in accordance with the guidelines of the University of Alabama at Birmingham Institutional Animal Care and Use Committee.

2.2. Pancreatic mass index, glucose physiology, and islet isolation

At P1, pancreata were collected, weighed for pancreatic mass index calculation (pancreas weight/total body weight × 100 [20]), and formaldehyde fixed for histology. Trunk blood was collected from P1 and P10 mice and blood glucose measured using an automatic glucometer (Bayer Contour Next). Mice P21 and older were fasted for six hours prior to glucose measurements from the tail vein. Glucose tolerance tests (GTTs) were performed as previously described [29] with a glucose dosage of 2.5 g/kg body weight. For GSIS and RNA analyses, islets were isolated from 14-week $SSBP3^{\Delta\beta\text{-}cell}$ and littermate CTL mice using a standard collagenase digestion method followed by hand picking [30].

2.3. Static glucose stimulated insulin secretion (GSIS)

Isolated islets were preincubated in Krebs Ringer Buffer (KRB — 118.4 mM NaCl, 4.69 mM KCl, 1.18 mM $MgSO_4$, 1.18 mM KH_2PO_4, 25 mM $NaHCO_3$, 5 mM N-2-hydroxyethylpiperazine-N-2-ethane sulfonic acid, 2.52 mM $CaCl_2$, pH 8.4) supplemented with 2.8 mM glucose and 0.5% fatty acid free bovine serum albumin for 45 min. Five islets were placed into each well of a 96-well plate and incubated in 100 μL of KRB supplemented with 2.8 mM glucose (low) or 16.7 mM glucose (high) for 45 min. The supernatants were collected for quantification of secretion, which was normalized to insulin content. For insulin content, islet pellets were lysed in 200 μL of lysis buffer (100 mM Tris—HCl, pH 8.0; 300 mM NaCl; 10 mM NaF; 2 mM Na_3VO_4; 2% NP-40; Protease inhibitor cocktail tablet [Roche, 1 tablet/25 mL]). Insulin was measured using the Ultrasensitive Mouse Insulin ELISA kit, according to manufacturer's instructions (Crystal Chem, #90080) [31].

2.4. Plasma insulin measurements

Fasted control and $SSBP3^{\Delta\beta\text{-}cell}$ mice were subjected to glucose challenge (described above) and tail vein blood was collected at time = 0 and 15 min after glucose injection. Plasma was isolated from tail blood samples followed by insulin ELISA (Crystal Chem, #90080).

2.5. RNA isolation, cDNA synthesis, and qPCR analysis

RNA was isolated from P1 whole pancreas and 14-week islets in SSBP3 knockout and littermate CTL animals using an RNeasy Micro Kit (Qiagen, #74004) and cDNA was synthesized using the iScript cDNA kit (Bio-Rad, #170-8840). qPCR was performed in duplicate using iTaq SYBR Green (Bio-Rad, #172-8840) and Bio-Rad CFX96 C1000 Touch Real-Time PCR Detection System. Data was analyzed by the $2^{-\Delta\Delta\ CT}$ method and normalized to *gapdh* as the housekeeping gene. Primer sequences can be found in Supplemental Table 1.

2.6. Immunohistochemical analysis and quantification

Neonatal and adult pancreata were dissected, fixed in 4% formaldehyde/PBS for 4—6 h, then paraffin embedded. Sections were cut to 6 μm using a Leica RM2235 microtome and blocked using 5% normal donkey serum (Jackson ImmunoLabs) in 1% bovine serum albumin/PBS for 1 h at room temperature. Slides were incubated with primary antibodies at 4 °C overnight (antibodies and dilutions in Supplemental Table 2). Secondary antibodies were incubated for 2 h at room temperature, then slides were mounted using DAPI Fluoromount G mounting medium (Southern Biotech # 0100-20). Imaging was performed using a Zeiss LSM710 confocal microscope and processed by Zen Software (Zeiss). For quantification of islet cell types, all Pax6+ cells were counted in four sections per mouse, at least 30 μm apart (over 17,200 total cells counted) [10]. For α-cell quantification, $glucagon^{+}/Pax6^{+}$ cells were counted (and represented over $Pax6^{+}$ in Figure 2E). For non-β cell quantification, the insulin-negative/$Pax6^{+}$ cells were counted to represent other islet cell types (including α, δ, ε, and PP). Non-β cells were also represented over $Pax6^{+}$. Representative images of the stains used for quantification are included in Supplemental Figure 5. For quantification of percent islet hormone area (Figure 2F), P10 CTL and $SSBP3^{\Delta Islet}$ pancreas tissues were stained for insulin or glucagon, as above, and the $hormone^{+}$ cell area was quantified from three biological replicates (three non-overlapping sections from each) as a percentage of total pancreas area using ImageJ (NIH).

2.7. Library preparation and RNA-Seq analyses

Total islet RNA was collected as described above and RNA-Seq library preprocessing and sequencing were performed with 3 CTL ($SSBP3^{F/F}$) and 3 $SSBP3^{\Delta\beta\text{-}cell}$ whole-islet RNA samples by the UAB Genomics Core. Paired-end sequence data were extracted in FastQ format.

Isl1-and Ldb1-depleted and CTL transcriptomic datasets were extracted from Ediger et al. [16] (Geo Accession: GSE84759) and analyzed in parallel with $SSBP3^{\Delta\beta\text{-}cell}$ samples. FastQ files underwent quality control with FastQC v0.11.9 [32], raw sequencing data was trimmed for low-quality reads, short reads, and adaptor sequences with Trim Galore v0.6.7 software [33], followed by an additional QC with FastQC. With STAR v2.7.3a [34], the trimmed reads were aligned to the GRCm39 genome for exons and were converted to Bam files. Read counts were generated with FeatureCounts through Rsubread v2.12.3 [35], using the Ensembl GTF annotations (GRCm39.109.gtf). Counts were processed by DEseq2 v1.38.3 [36] for differential gene expression. For sample quality control, principal component analysis (PCA) and hierarchical unsupervised clustering of global expression was performed and the following samples were chosen for

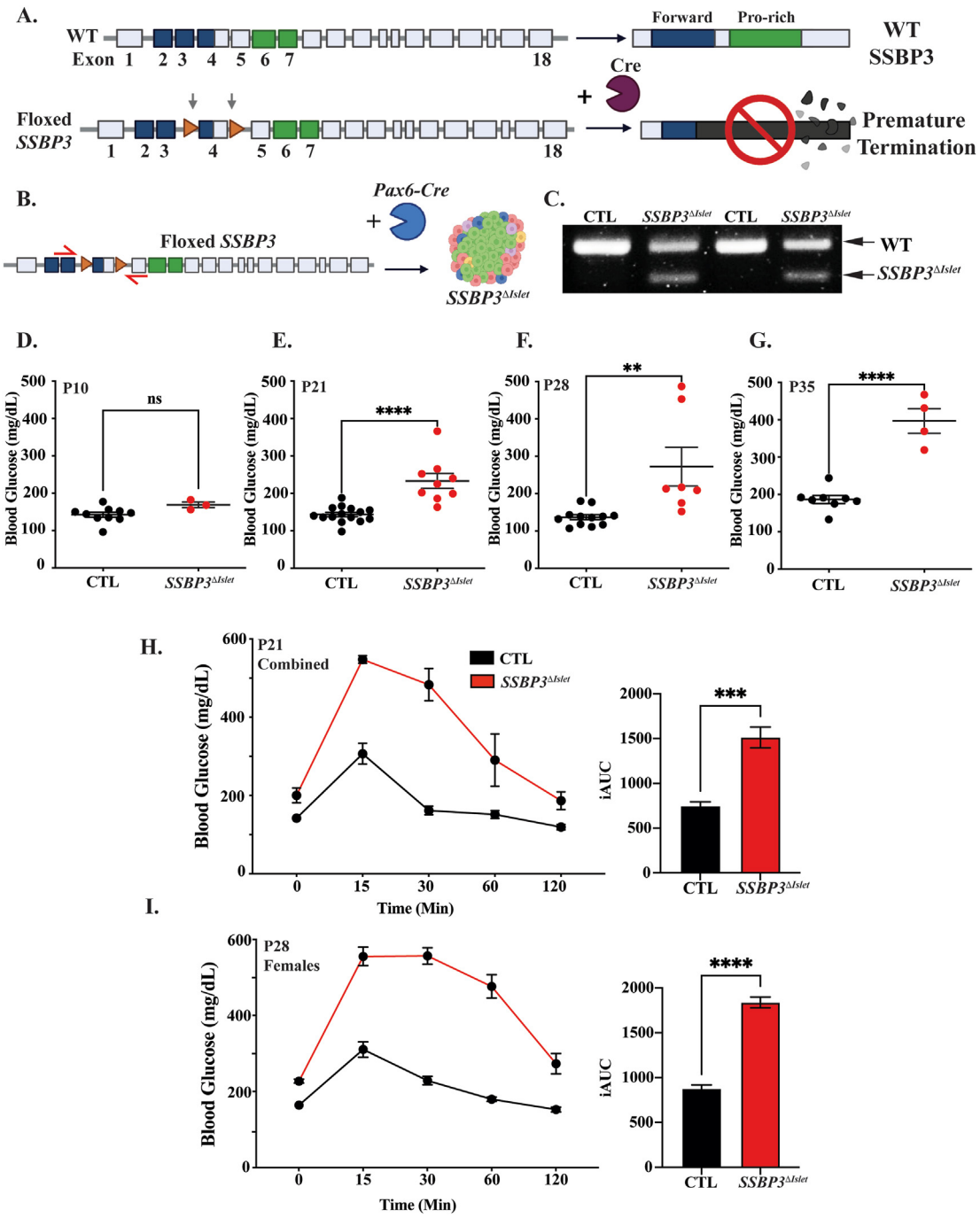

Figure 1: Generation of *SSBP3*$^{\Delta Islet}$ mouse model and assessment of glucose homeostasis. A) Schematic detailing the generation of the *SSBP3* floxed allele. In the WT, exons 2, 3, and 4 of the 18-exon gene encode the Ldb1-interacting FORWARD domain (blue) and exons 6 and 7 encode the proline-rich domain (Pro-rich, green). Floxed *SSBP3* has LoxP sites (orange) flanking exon 4 and Cre-mediated recombination results in a predicted frameshift and premature termination. B) *SSBP3*$^{\Delta Islet}$ knockout strategy using islet-specific *Pax6-Cre*. Red arrows indicate location of RT-PCR primers. C) Floxed exon 4 excision confirmed by RT-PCR in mRNA from isolated islets at P28. Top band (234 bp) is the WT product, bottom band (150 bp) represents *SSBP3*$^{\Delta Islet}$ RNA products lacking exon 4. D) At P10 *SSBP3*$^{\Delta Islet}$ mice (red) show no significant differences in *ad lib* blood glucose compared to littermate CTLs (black), n = 3–10, males and females. E–F) By P21 and P28 *SSBP3*$^{\Delta Islet}$ mice have significantly elevated fasting blood glucose, n = 7–15, males and females. G) *SSBP3*$^{\Delta Islet}$ female fasting blood glucose at P35, n = 4–8. H) Glucose tolerance test (GTT) in P21 male and female mice and significantly increased area under the curve (iAUC, right), n = 3–5. I) Female GTT at P28 and corresponding iAUC, n = 3–5. $^{**}P < 0.01$, $^{***}P < 0.001$, $^{****}P < 0.001$.

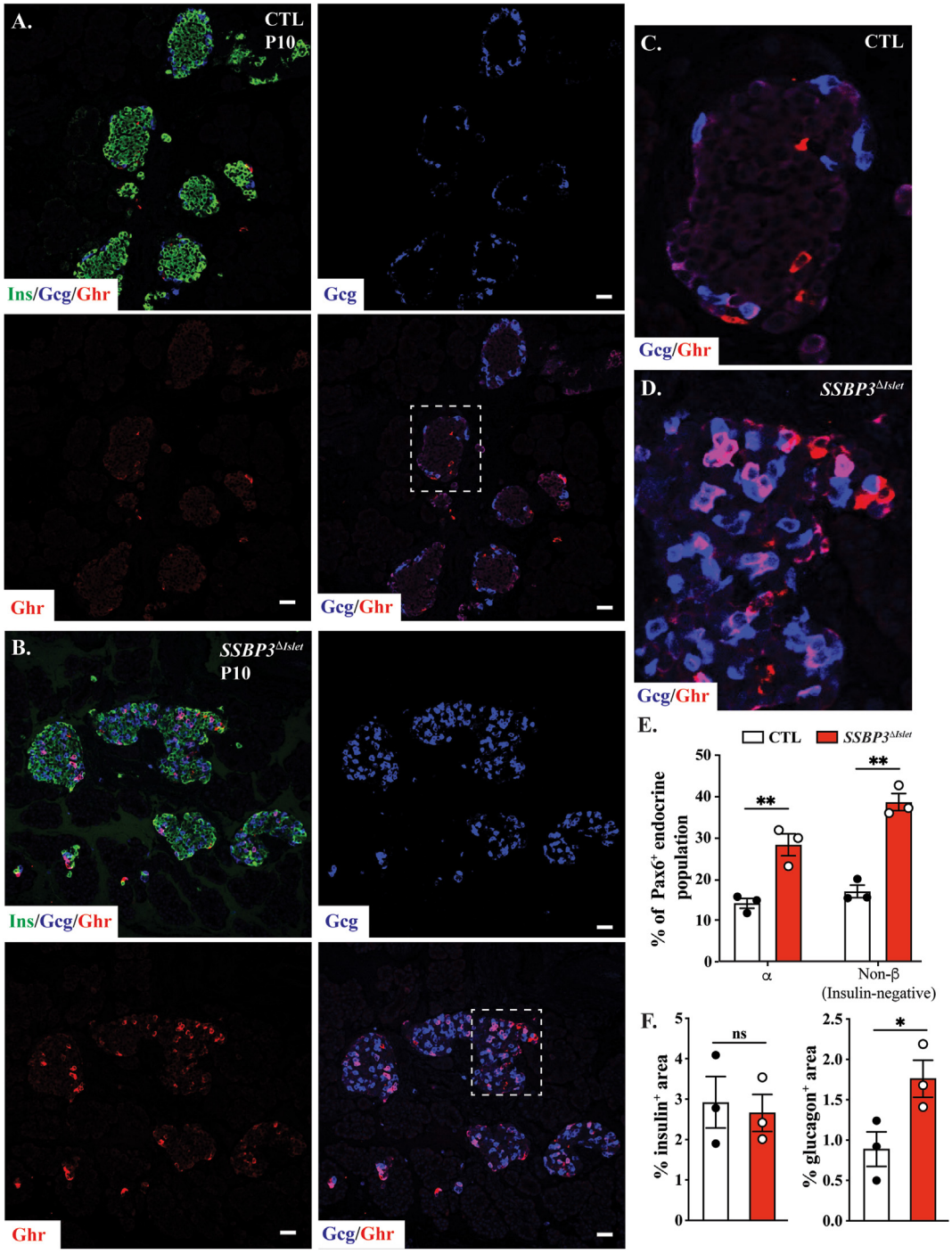

Figure 2: *SSBP3*$^{\Delta Islet}$ mice exhibit islet architecture defects and altered ratios of islet cell types. A) Immunofluorescence for insulin (green), glucagon (blue), and ghrelin (red) shows typical rodent pattern of glucagon-producing α-cells on the periphery and very few detectible ghrelin$^+$ ε-cells. B) *SSBP3*$^{\Delta Islet}$ islets exhibit increased glucagon$^+$ and ghrelin$^+$ cells. Glucagon$^+$ α-cells (blue) are highly abundant throughout the islet area. C–D) Magnified insets of CTL and *SSBP3*$^{\Delta Islet}$ images from A–B (hatched boxes) highlight glucagon/ghrelin co-positive cells. Scale bars = 20 μM. E) Quantification of endocrine (Pax6$^+$) cells in control (white bars) and knockout (red bars) mice indicates a significant increase in α- (Pax6$^+$/glucagon$^+$) and non-β (Pax6$^+$/insulin$^-$) cells in *SSBP3*$^{\Delta Islet}$ islets. F) Islet morphometry of % insulin$^+$ (left) or glucagon$^+$ (right) area in CTL and *SSBP3*$^{\Delta Islet}$ pancreata. n = 3 biological replicates with 3 non-overlapping sections averaged from each. $^*P < 0.05$; ns, not significant. n = 3, $^{**}P < 0.01$.

comparison: *SSBP3*$^{\Delta\beta\text{-}cell}$ and CTLs (Geo Accession: GSE232750), *Isl1* and *Ldb1* controls (SRR3948070, SRR3948071, SRR3948073, SRR3948074), *Isl1*-depleted (SRR3948057, SRR3948058, SRR3948059, SRR3948060, SRR3948061), and *Ldb1*-depleted (SRR3948062, SRR3948063, SRR3948064, SRR3948065, SRR3948066, SRR3948067, SRR3948068, SRR3948069).

Unsupervised hierarchical cluster analysis was performed with pheatmap v1.0.12 [37] to visualize the global gene expression pattern.

Pathway over-representation analysis was performed with the hypergeometric model-based program, clusterProfiler v4.6.0 for GO [38,39]. All graphs were made with ggplot2 v3.40 [40].

2.8. Statistical analysis

All data are represented as mean ± SEM. Statistical significance was determined using a Student's *t*-test or a two-way ANOVA, followed by *post hoc* analysis using GraphPad Prism statistical software (version 9.3). A *P*-value of 0.05 or less was considered significant.

3. RESULTS

3.1. SSBP3-deficient neonates are hyperglycemic and glucose intolerant

To assess *in vivo* roles of pancreatic SSBP3, we generated a novel mouse with LoxP sites flanking exon 4 (Supplemental Figure 1), which partially encodes the Ldb1-interacting FORWARD domain [25] (Figure 1A). As a consequence of exon 4 recombination, a frameshift is predicted in exon 5 yielding a premature termination codon (PTC) in exon 6 of the mutant protein. Thus, we expect any translated fragment of mutant SSBP3 to lack functional FORWARD and proline-rich domains. We first used the *Pdx1-Cre* line to generate $SSBP3^{\Delta Panc}$ mice (*Pdx1-Cre*; $SSBP3^{F/F}$, Supplemental Figure 3A) and because commercial SSBP3 antibodies used in our prior publication are no longer available, we used RT-PCR to visually demonstrate Cre-mediated *SSBP3* recombination in RNA from whole pancreata (Supplemental Figure 3A, bottom). The faster migrating band indicates exon 4 excision. We found that *ad lib* fed P1 $SSBP3^{\Delta Panc}$ mice were significantly hyperglycemic with no change in pancreas size (Supplemental Figure 3B–C). Preliminary mRNA analysis of whole pancreata at P1 revealed trends toward decreased expression of Ldb1 targets, *MafA* and *Hb9* (also called *Mnx1*, [19]; Supplemental Figure 3D). The trending increase in *ghrelin* observed here was interesting and was explored further in the islet-specific model below. These $SSBP3^{\Delta Panc}$ data support a role for SSBP3 in glucose homeostasis and islet cell development. Due to our interest specifically in the islet, and reported mosaicism of the *Pdx1-Cre* [41], we developed an islet-specific model using a *Pax6*-driven *Cre* transgene, the same Cre line used to recombine *Ldb1* in a previous study [19].

We generated the $SSBP3^{\Delta Islet}$ model (Figure 1B) and confirmed *SSBP3* recombination in P28 islets using the RT-PCR method described above (primer locations in exons 3 and 5 indicated by red arrows, Figure 1B–C). At P10, we measured *ad lib* blood glucose in males and females and did not observe a difference (Figure 1D). However, by P21 and P28 (Figure 1E–F) $SSBP3^{\Delta Islet}$ fasting blood glucose (combined sexes) was significantly elevated compared to littermate CTLs and heterozygotes (*Pax6-Cre*; $SSBP3^{F/+}$, data not shown). Males were sacrificed by P28 due to severe hyperglycemia, and P35 females remained significantly hyperglycemic (Figure 1G). GTTs conducted with combined P21 males and females indicated glucose intolerance by significant increase of area under the curve in $SSBP3^{\Delta Islet}$ mice (Figure 1H). P28 females exhibited severe glucose intolerance (Figure 1I). These findings support that SSBP3 has a significant role in islet glucose homeostasis in male and female mice.

3.2. $SSBP3^{\Delta Islet}$ mice exhibit islet architecture defects and increased non-β islet cell numbers

At P10, we assessed islet hormones by immunofluorescence (IF). Unlike normal peripheral expression in CTL islets (Figure 2A, blue), $SSBP3^{\Delta Islet}$ islets exhibited striking penetration of glucagon$^+$ cells into the islet core, as well as an overall increase in glucagon$^+$ cells (Figure 2B, blue). We investigated ghrelin by IF and found what appeared to be abnormally increased ghrelin$^+$ cells in $SSBP3^{\Delta Islet}$ islets (Figure 2B, red). Loss of the Nkx2.2 TF is known to impart increased islet ghrelin$^+$ ε-cells [42], however we detected no overt change in Nkx2.2 expression in $SSBP3^{\Delta Islet}$ islets (Supplemental Figure 4). These data suggest SSBP3 may regulate ε-cell number/ghrelin expression through an Nkx2.2-independent mechanism.

In CTLs, glucagon/ghrelin co-positive cells were observed, and are known to exist in normal islets (Figure 2C, [43]), but IF revealed an apparent increase in these co-positive cells in $SSBP3^{\Delta Islet}$ animals (Figure 2C, D). Quantification of glucagon/Pax6 co-positive cells confirmed a significant increase in α-cells (Figure 2E). To represent α, ε, and other non-β islet cells, we counted insulin-negative/Pax6$^+$ cells (quantification method depicted with representative images in Supplemental Figure 5) and observed a significant increase in 'non-β' endocrine cells as well (Figure 2E, right). This phenotype was also observed at P21 (data not shown). We also assessed insulin$^+$ and glucagon$^+$ cell area as a percentage of total pancreas area in the P10 control and $SSBP3^{\Delta Islet}$ tissue samples (Figure 2F). We observed no change in β-cell area, but an increase of α-cell area supporting the cell quantification in Figure 2E, above. These data suggest a role for SSBP3 in islet cell fate, where loss appears to disrupt not only islet architecture, but perhaps allocation into expected α, β, δ, ε, and PP endocrine cell ratios.

3.3. SSBP3 loss disrupts MafA expression

One hallmark of β-cell maturation and proper GSIS is expression of the TF gene *MafA*, which is a known target of LIM-complex partners Ldb1 and Isl1 [10,19]. In CTL E18.5 embryos, most insulin-producing cells express MafA (Figure 3A, white nuclei), while E18.5 $SSBP3^{\Delta Islet}$ islets exhibit defects in islet architecture and contain insulin$^+$ cells lacking MafA expression (Figure 3B, white arrows). At P10, this phenotype is maintained, with many insulin$^+$ or Nkx6.1$^+$ β-cells in $SSBP3^{\Delta Islet}$ islets lacking MafA, unlike littermate CTLs (Figure 3C–E). Co-staining with β-cell TF Nkx6.1 shows that many MafA-deficient cells maintain Nkx6.1 expression, providing potential specificity to *MafA* as an SSBP3 target *in vivo*.

3.4. $SSBP3^{\Delta Islet}$ β-cells lack key functionality and identity markers

The significant blood glucose defect observed in $SSBP3^{\Delta Islet}$ mice (Figure 1D–I) prompted investigation of other markers of β-cell function and identity. Assessment of a functional maturity marker UCN3, the key β-cell TF Pdx1, and Glut2 glucose transporter at P21, revealed all three markers to be strikingly reduced in $SSBP3^{\Delta Islet}$ mice (Figure 4). Glut2 was nearly absent in $SSBP3^{\Delta Islet}$ β-cells (Figure 4E–F, bottom) and MafA was undetectable by this age (Figure 4F). These defects indicate that, in addition to the islet-wide defects observed in Figure 2, SSBP3 also plays a critical role in maintenance of β-cell function and identity.

3.5. β-Cell SSBP3 is required for glucose homeostasis and GSIS

To bypass any developmental/neonatal SSBP3 contributions and considering requirement of binding partners Isl1 and Ldb1 for adult β-cell function [16], we aimed to assess the role of SSBP3 specifically in the adult β-cell. We generated a tamoxifen-inducible SSBP3 knockout model, termed $SSBP3^{\Delta\beta\text{-}cell}$ (Figure 5A). Exon 4 excision was again confirmed by RT-PCR (Figure 5B) and qPCR also supported a significant reduction of *SSBP3* mRNA (Figure 5C) in islets isolated from 14-week-old mice. Tamoxifen was administered by oral gavage every other day starting at 4-weeks until 6-weeks of age to recombine *SSBP3* exon 4 specifically in adult β-cells (Figure 5D). $SSBP3^{\Delta\beta\text{-}cell}$

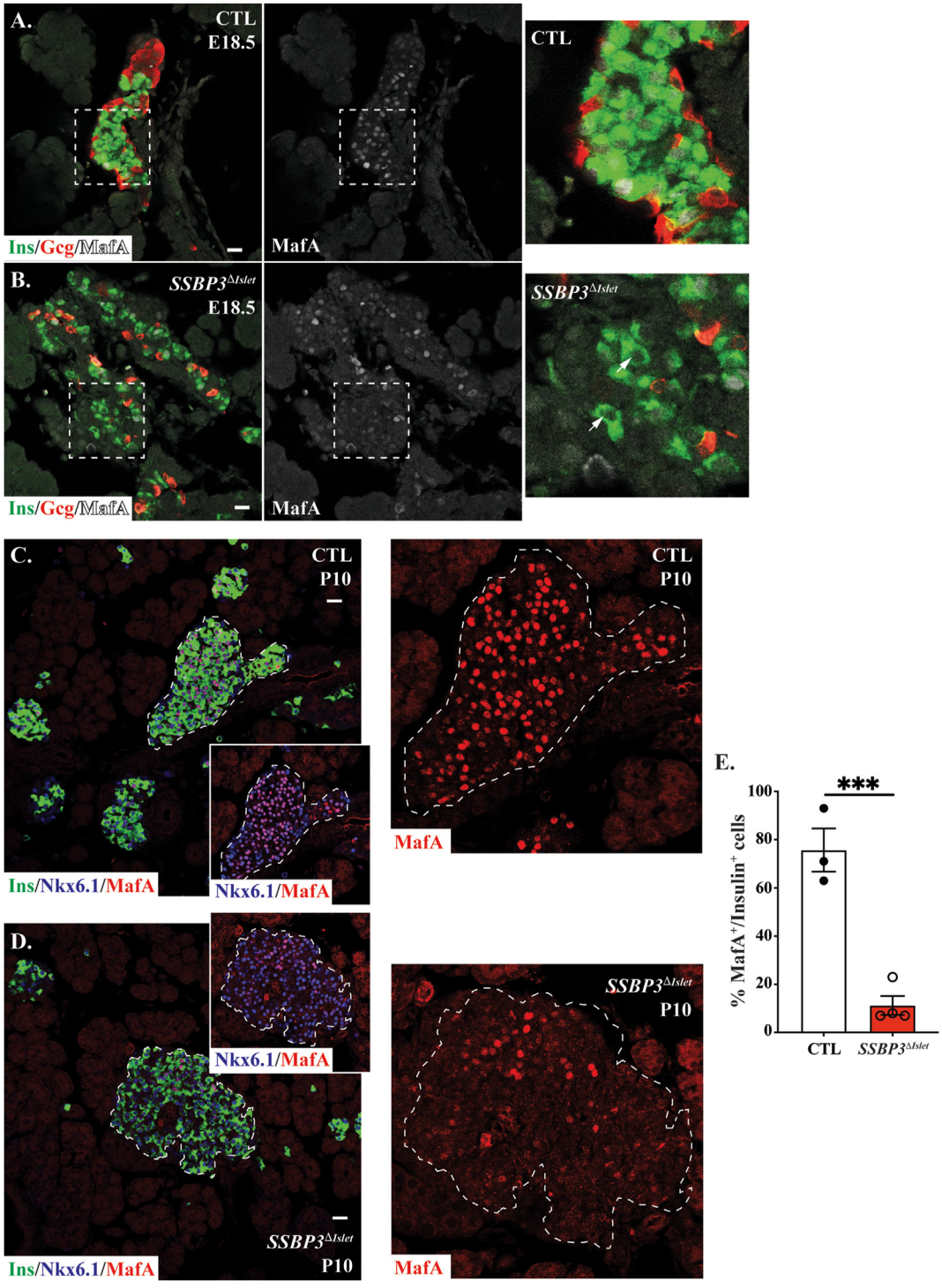

Figure 3: MafA is disrupted by SSBP3 loss *in vivo*, as early as E18.5. A) Endocrine clusters in E18.5 CTL mice exhibit insulin (green) and MafA (white) co-expressing cells and a typical β-cell core, α-cell mantle architecture. B) Many embryonic *SSBP3*$^{\Delta Islet}$ β-cells are lacking MafA (white arrows, right) and core/mantle architecture appears disrupted. C–D) CTL islets in P10 neonates express Nkx6.1 (blue) and MafA (red) within the insulin^{+} area (white dashed line). D) *SSBP3*$^{\Delta Islet}$ islets maintain insulin and Nkx6.1 expression, but MafA is largely absent from the islet area. Higher magnification images of MafA staining are also shown at the right. Scale bar = 20 μM. E) Quantification of MafA and insulin co-expressing cells as a percentage of total insulin^{+} β-cells in CTL (white bars) and *SSBP3*$^{\Delta Islet}$ (red bars) pancreas samples. Cell counts were averaged from three biological replicates of each genotype. $^{***}P < 0.0001$.

male mice were hyperglycemic compared to littermate CTL s at 6-, 8-, and 10-weeks old (Figure 5E–G). Female *SSBP3*$^{\Delta\beta\text{-cell}}$ mice did not have a phenotype distinguishable from CTLs (Supplemental Figure 2), thus only males were used for subsequent analyses. *SSBP3*$^{\Delta\beta\text{-cell}}$ mice were glucose intolerant by 8-weeks of age (data not shown) through 14-weeks (Figure 5H), at which point they were sacrificed. Plasma collection at 0- and 15-minutes post-glucose injection revealed reduced plasma insulin during a GTT (Figure 5I). Isolated

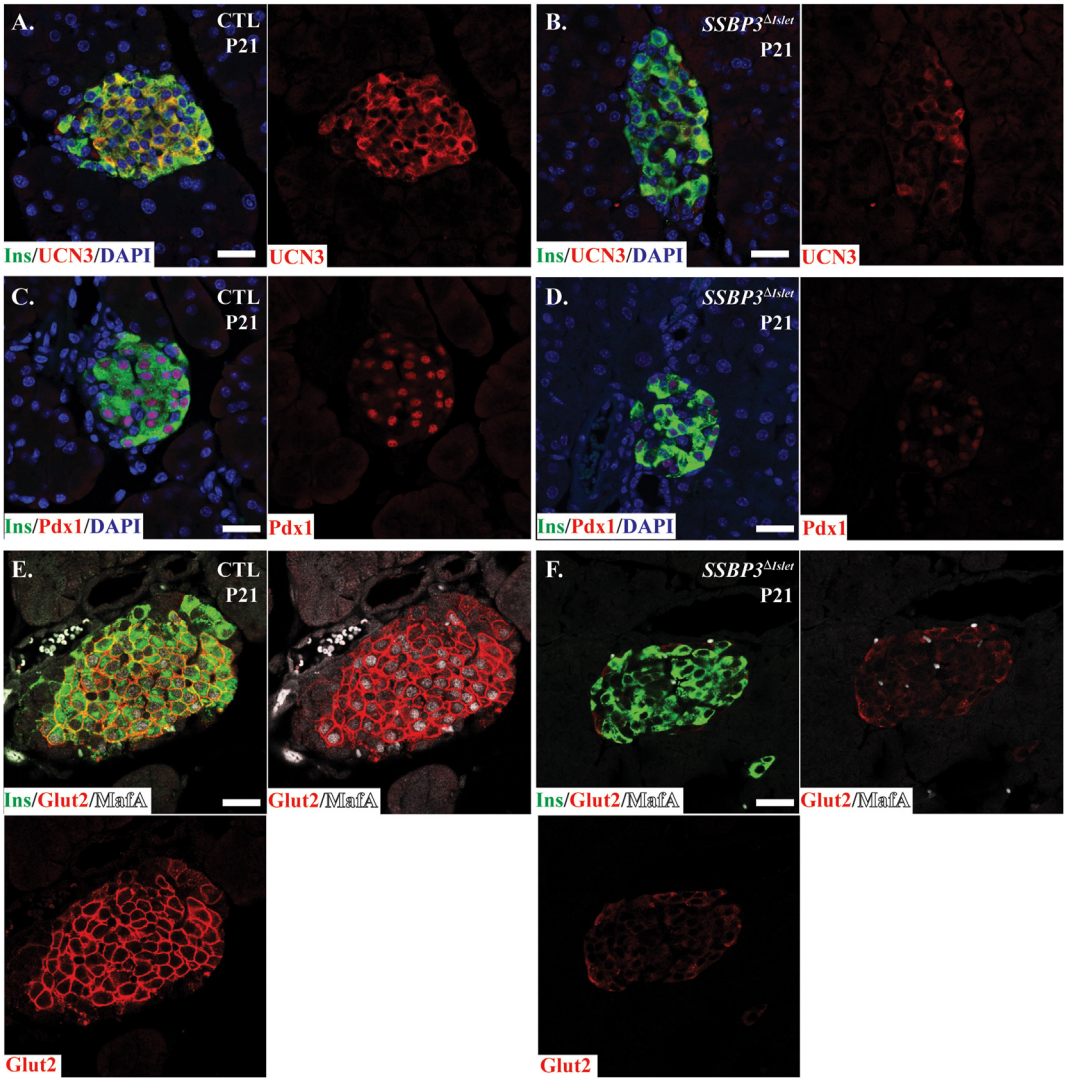

Figure 4: *SSBP3*$^{\Delta Islet}$ β-cells lack key functionality and identity markers. Immunofluorescence staining for insulin and UCN3 in P21 CTL (A) and *SSBP3*$^{\Delta Islet}$ (B) mice highlights a striking loss of UCN3 expression in *SSBP3*$^{\Delta Islet}$ β-cells. C–D) CTL insulin^{+} β-cells co-stain for Pdx1 (red), but in *SSBP3*$^{\Delta Islet}$ mice insulin^{+} β-cells exhibit reduced Pdx1 levels. E–F) CTL β-cells display normal cell-surface pattern for Glut2 (red) and nuclear MafA (white). In *SSBP3*$^{\Delta Islet}$ islets, Glut2 is greatly reduced and MafA is absent in *SSBP3*$^{\Delta Islet}$ tissue. Scale bar = 20 μM.

islets from 14-week-old *SSBP3*$^{\Delta\beta\text{-cell}}$ mice had unchanged insulin content (Figure 5J), but upon stimulation with high glucose (16.7 mM), we observed a significant reduction of insulin secretion compared to CTLs (Figure 5K). These data highlight that SSBP3 is required for glucose tolerance and GSIS responses from the β-cell.

3.6. Adult β-cell function and identity markers are disrupted by inducible SSBP3 loss

Immunofluorescence of 14-week-old male control and *SSBP3*$^{\Delta\beta\text{-cell}}$ pancreata suggested a reduction of the β-cell maturity marker UCN3 at the islet periphery and reduced Pdx1 levels throughout the islet (Figure 6A–B). While Glut2 was present in these islets (unlike in *SSBP3*$^{\Delta Islet}$ mice, Figure 3), peripheral β-cells had an abnormal subcellular Glut2 localization (Figure 6C–D, white arrows). qPCR analysis in 14-week isolated islets demonstrated a reduction of *Glut2*, *MafA*, and *Pdx1*. These data highlight a role for SSBP3 in maintaining key drivers of β-cell identity and function.

3.7. Transcriptomic analysis reveals shared gene targets between SSBP3, Ldb1, and Isl1

To comprehensively investigate the transcriptional impacts of *SSBP3* loss in adult β-cells, we performed RNA-sequencing on whole islets isolated from male control and *SSBP3*$^{\Delta\beta\text{-cell}}$ mice at 14-weeks of age (Figure 7). Using a padj <0.05, we found 1082 downregulated and 998 upregulated differentially expressed genes (DEGs) in *SSBP3*$^{\Delta\beta\text{-cell}}$ islets, which can be visualized by clustering in the heatmap and PCA plots (Figure 7A–B). Read counts for *SSBP3* also confirm reductions in the *SSBP3*$^{\Delta\beta\text{-cell}}$ model (Figure 7C). Over-representation analysis revealed a significant enrichment for biological processes involved in chromatin remodeling and cell fate specification, which suggests candidate pathways involved in the development of the SSBP3 knockout phenotypes (Figure 7D, top). Protein-containing complex disassembly was also upregulated, supporting the known role of SSBP3 as a LIM-complex stabilizer. Gene sets associated with peptide hormone metabolism,

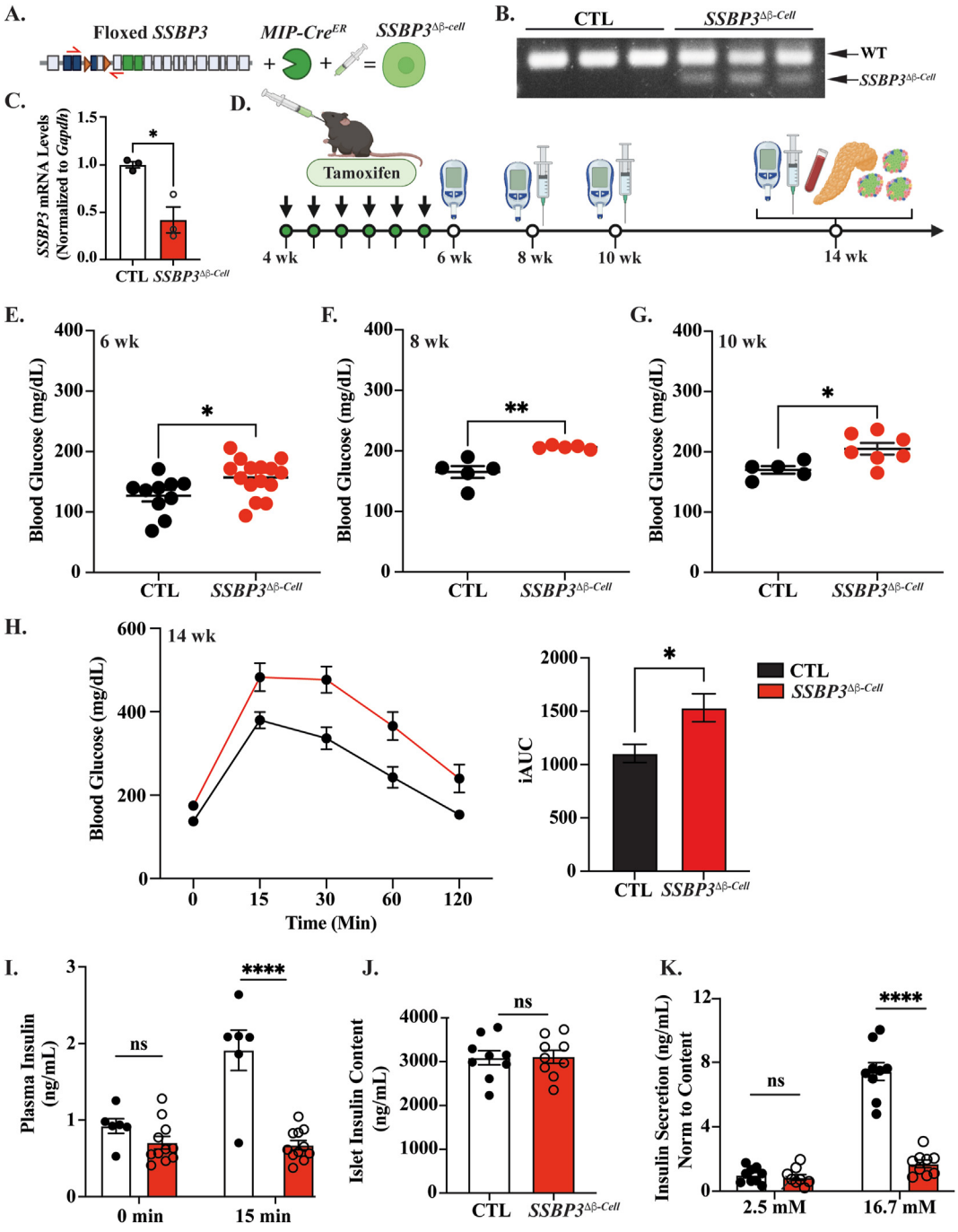

Figure 5: Inducible SSBP3 loss demonstrates a requirement for adult β-cell function. A) Schematic for generation of *SSBP3*$^{\Delta\beta\text{-cell}}$ mice using tamoxifen-inducible *MIP-Cre*^{ER}. Red arrows represent locations of RT-PCR primers. B) Confirmation of Cre-mediated recombination using RT-PCR and gel electrophoresis from 14-week whole-islet RNA. Black arrows indicate WT and *SSBP3*$^{\Delta\beta\text{-cell}}$ bands. C) Reduction of *SSBP3* mRNA in *SSBP3*$^{\Delta\beta\text{-cell}}$ islets at 14-weeks by qPCR, n = 3. D) Experimental design for *SSBP3*$^{\Delta\beta\text{-cell}}$ model, details in methods. Briefly, induction regimen began at 4-weeks of age and fasting blood glucose, GTT, plasma collection, islet isolation, and pancreas histology were conducted at the indicated time points. E–G) *SSBP3*$^{\Delta\beta\text{-cell}}$ mice (red) are hyperglycemic compared to littermate CTLs (black) at 6-, 8-, and 10-weeks, n = 5–15 per group. H) GTT at 14-weeks (left). *SSBP3*$^{\Delta\beta\text{-cell}}$ mice are glucose intolerant as indicated by significantly increased area under the curve (iAUC, right), n = 8–9. I) *In vivo* GSIS at 0- and 15 min post-glucose challenge at 14-weeks. *SSBP3*$^{\Delta\beta\text{-cell}}$ mice have reduced plasma insulin levels at 15 min. J) Insulin content was unchanged between CTL and knockout islets. K) Static GSIS in isolated islets from 14-week-old mice demonstrates reduced insulin secretion at high glucose (16.7 mM) in *SSBP3*$^{\Delta\beta\text{-cell}}$ mice. $^{*}P < 0.05$, $^{**}P < 0.01$, $^{****}P < 0.0001$.

oxidative phosphorylation, and ATP metabolism were downregulated (Figure 7D, bottom), strongly supporting the observed glucose metabolism dysfunction phenotypes. Selected genes of interest related to β-cell function and identity including *MafA*, *Ucn3*, *Ins1*, *Ins2*, *G6pc2*, and *Gipr* were reduced (Figure 7E–F). Interestingly, we found reductions in the mRNA encoding LIM-only factor, Lmo1, which may indicate an SSBP3-mediated role for Lmo1 in the β-cell. Upregulated *SSBP3*$^{\Delta\beta\text{-cell}}$ islet mRNA included several markers of β-

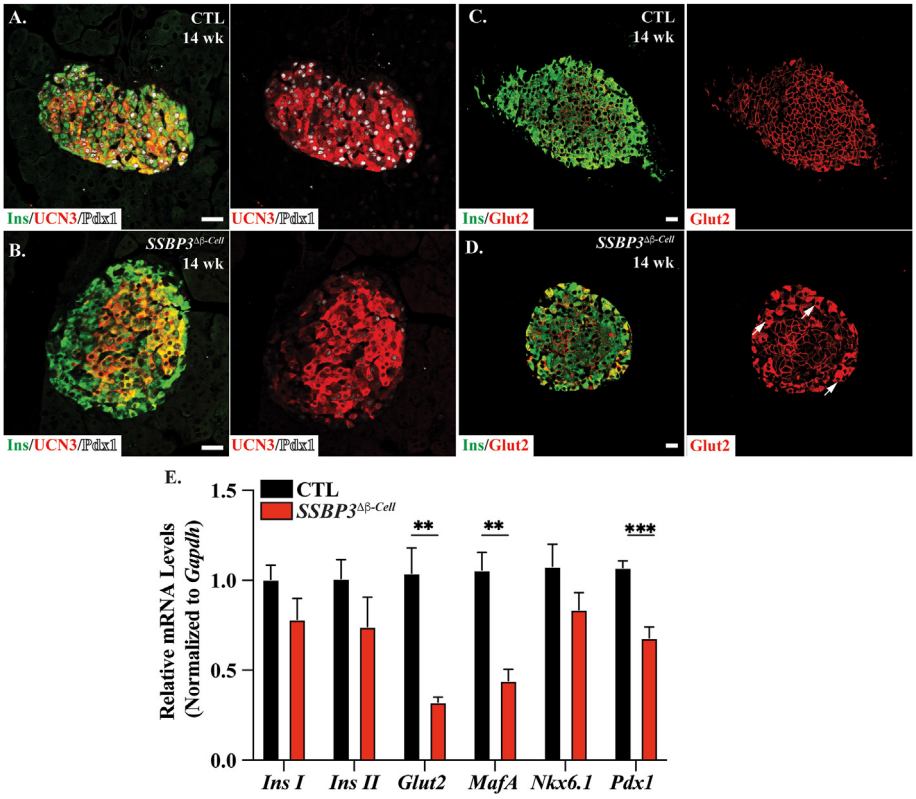

Figure 6: *SSBP3*$^{\Delta\beta\text{-cell}}$ mice exhibit reductions in β-cell functional identity markers. A) At 14-weeks, CTL mice express maturity marker UCN3 (red) throughout the insulin^{+} area and robust nuclear expression of the Pdx1 TF (white). B) The *SSBP3*$^{\Delta\beta\text{-cell}}$ model presents with peripheral UCN3 loss and Pdx1 reductions. C–D) Glut2 expression (red) outlines the β-cells in CTL animals (top), β-cells in *SSBP3*$^{\Delta\beta\text{-cell}}$ have abnormal cytoplasmic Glut2 localization (white arrows, bottom), particularly in peripheral β-cells. E) qPCR in 14-week isolated islets demonstrates decreased mRNA encoding Glut2, MafA, and Pdx1 in *SSBP3*$^{\Delta\beta\text{-cell}}$ islets. n = 4, $^{**}P < 0.01$. $^{***}P < 0.001$. Scale bar = 20 μM.

cell stress and dedifferentiation including *TXNIP*, *Aldh1a3*, and *Neurog3*.

Lastly, we wanted to compare SSBP3 DEGs to published β-cell Ldb1 and Isl1 knockout transcriptomic datasets (Figure 7G, [16]). We found 106 upregulated and 50 downregulated genes shared between all three factors of interest (selected shared DEGs in Figure 7G, right, full list in Supplemental Table 3). *Lmo1* and *MafA* were shared amongst genes downregulated in *SSBP3*, *Ldb1*, and *Isl1* knockouts as were β-cell genes *G6pc2* and *Pcsk1*. Shared upregulated genes include *Neurog3* and *Tph1*, as well as those encoding β-cell TF Rfx6 and the fetal islet hormone gastrin, which has been linked to diabetes-induced β-cell reprogramming [44]. These relationships require further study to determine mechanisms, but our data solidifies a role for SSBP3 as a driver of β-cell function and identity and establishes potential new molecular candidates for SSBP3 interactors and downstream targets.

4. DISCUSSION

In this study, we reveal critical roles for the SSBP3 transcriptional co-regulator in the mouse pancreas that build on our previously published *in vitro* work identifying SSBP3 as an interactor of Isl1 and Ldb1 in the β-cell [21]. Here, we developed a novel *SSBP3* LoxP allele mouse paired with various Cre-driver lines to demonstrate that islet development and glucose homeostasis require SSBP3. Loss of pancreas- (*Pdx1-Cre*) or islet-wide (*Pax6-Cre*) *SSBP3* caused significant hyperglycemia as early as P1 (Supplemental Figure 3, Figure 1). MafA expression was reduced in β-cells as early as E18.5, prior to potential secondary glucotoxicity effects (Figure 3). Islets in *SSBP3*$^{\Delta Islet}$ mice exhibited striking architecture abnormalities and an increase in α- and other non-β islet cells, despite no change in insulin^{+} cell area (Figure 2). To bypass potential developmental defects, the inducible *SSBP3*$^{\Delta\beta\text{-cell}}$ model revealed, in addition to hyperglycemia and glucose intolerance, drastic reductions in plasma insulin during a glucose challenge and GSIS from isolated islets *ex vivo* (Figure 5). Glucose intolerance and loss of β-cell identity factors appeared to be more extreme in the developmental *SSBP3*$^{\Delta Islet}$ compared to the *SSBP3*$^{\Delta\beta\text{-cell}}$ model. For example, *SSBP3*$^{\Delta Islet}$ β-cells exhibited a near complete loss of MafA, Pdx1, Glut2, and UCN3 by IF (Figure 4). This variation may be due to technical differences in *Pax6*-versus *MIP-Cre*^{ER} recombination efficiency, but perhaps aging *SSBP3*$^{\Delta\beta\text{-cell}}$ mice further after induction would yield similarly drastic defects. We observed sex differences in these SSBP3-deficient models where *SSBP3*$^{\Delta Islet}$ females had a slightly delayed (albeit still severe) glucose tolerance phenotype, while *SSBP3*$^{\Delta\beta\text{-cell}}$ females remained glucose tolerant. These results are consistent with published sex asymmetry in diabetes and glucose metabolism [45,46]. Despite these minor divergences between models, both *SSBP3*$^{\Delta Islet}$ and *SSBP3*$^{\Delta\beta\text{-cell}}$ mice clearly exhibit a necessity for SSBP3 in islet β-cell function.

Further supporting SSBP3 as a regulator involved in β-cell functional identity, *SSBP3*$^{\Delta Islet}$ and *SSBP3*$^{\Delta\beta\text{-cell}}$ mice exhibited defects in UCN3 expression (Figures 4, 6). "Virgin" β-cells are a UCN3-negative, immature, and relatively infrequent (1–2% of adult β-cells) population located on the islet periphery in wild type mice [47]. We show peripheral UCN3 reductions in the *SSBP3*$^{\Delta\beta\text{-cell}}$ model (Figure 6) that may

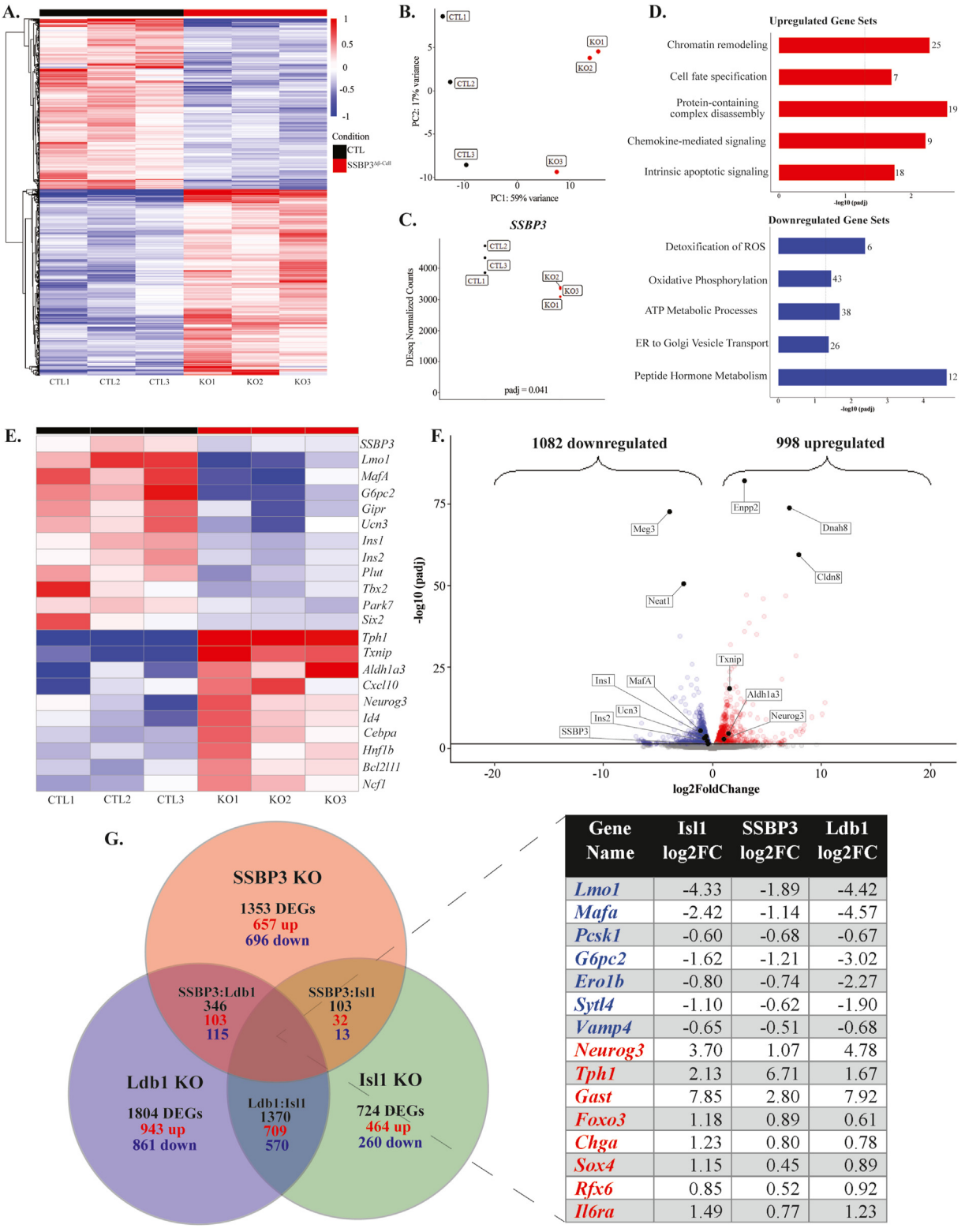

Gene Name	Isl1 log2FC	SSBP3 log2FC	Ldb1 log2FC
Lmo1	-4.33	-1.89	-4.42
Mafa	-2.42	-1.14	-4.57
Pcsk1	-0.60	-0.68	-0.67
G6pc2	-1.62	-1.21	-3.02
Ero1b	-0.80	-0.74	-2.27
Sytl4	-1.10	-0.62	-1.90
Vamp4	-0.65	-0.51	-0.68
Neurog3	3.70	1.07	4.78
Tph1	2.13	6.71	1.67
Gast	7.85	2.80	7.92
Foxo3	1.18	0.89	0.61
Chga	1.23	0.80	0.78
Sox4	1.15	0.45	0.89
Rfx6	0.85	0.52	0.92
Il6ra	1.49	0.77	1.23

Figure 7: β-Cell loss of *SSBP3* causes global gene expression changes similar to *Ldb1* and *Isl1*. A) Heatmap of all differentially expressed genes (DEGs) in islet RNA from $SSBP3^{\Delta\beta\text{-cell}}$ (red) and CTL (black) mice at 14-weeks (padj <0.05). B) PCA of $SSBP3^{\Delta\beta\text{-cell}}$ CTLs and knockouts. C) Read counts of *SSBP3* highlight significantly reduced expression in $SSBP3^{\Delta\beta\text{-cell}}$ islets. D) GO term over-representation analysis of upregulated (top, red) and downregulated pathways (bottom, blue). Numbers indicate the count of DEGs associated with each GO term. Dotted vertical line is at padj $= 0.05$. E) Selected genes of interest heatmap. F) Volcano plot of selected $SSBP3^{\Delta\beta\text{-cell}}$ DEGs. Blue represents downregulated, red represents upregulated, and gray represents genes without significant change, solid horizontal line at padj $= 0.05$. G) Venn diagram of DEGs between $SSBP3^{\Delta\beta\text{-cell}}$, published $Isl1^{-}$ and $Ldb1^{-}$ models. Table shows selected downregulated (blue) and upregulated (red) DEGs shared between all three models. Full list of shared DEGs in Supplemental Table 4.

represent an increase in virgin β-cells upon SSBP3 loss. Virgin β-cells are trans-differentiation intermediates between α- and β-cells, but we observed no overt increases of α-cells in *SSBP3*$^{\Delta\beta\text{-}cell}$ mice (data not shown). Future studies will determine if perhaps the significant increase of α-cells in *SSBP3*$^{\Delta Islet}$ mice (Figure 2) is a result of this trans-differentiation mechanism.

In addition to increased α-cells, we found an overt increase of ghrelin^{+} and glucagon^{+}/ghrelin^{+} cells in *SSBP3*$^{\Delta Islet}$ pancreata (Figure 2), which was also suggested by preliminary mRNA analysis in *SSBP3*$^{\Delta Panc}$ (Supplemental Figure 3). ε-Cell ghrelin regulation remains somewhat unexplained in the islet, but a recent zebrafish study demonstrated that extreme β-cell loss caused a Pax4-dependent increase in ε-cells [48]. These ε-cells were intermediates that would trans-differentiate into β-cells to replenish the lost mass. Further studies will investigate whether Pax4 is involved in our models, but perhaps SSBP3-deficient β-cell dysfunction is driving ε-cell increases. The Nkx2.2 TF is required for transcriptional repression of *ghrelin* in non-ghrelin producing islet cells [42], thus *Nkx2.2* null pancreata exhibited loss of β-cells and a striking increase in ghrelin [43], similar to our model. However, we found no changes in Nkx2.2 levels by IF (Supplemental Figure 4), suggesting an Nkx2.2-independent role for SSBP3 in affecting ε-/ghrelin^{+} cell levels.

Architecturally, the existence of numerous α- and ε-cells within the core of *SSBP3*$^{\Delta Islet}$ islets (Figure 2) may suggest a unique role for SSBP3 in the formation or migration of endocrine progenitors during development. Coordination of islet architecture and progenitor movement is still being uncovered, but islet cells that differentiate first are thought to exist on the islet periphery [49]. Fittingly, knockouts of the SSBP3-target gene *MafA* also feature islet architectural defects [50,51]. Perhaps SSBP3-mediated complexes have roles in endocrine progenitor fate, and also aspects of their cellular migration/localization during development.

In multiple tissue contexts, SSBP3 is an essential member of LIM-containing transcriptional complexes. Through association with the LCCD domain of Ldb1, SSBP3 prevents binding of the RLIM ubiquitin ligase and thus prohibits ubiquitin-mediated complex turnover [23]. SSBP3, Ldb1, and the LIM-HD TF Lhx1 coordinately regulate anterior/head development, where loss of each factor independently imparts a striking head-truncation phenotype [52–54]. We aimed to interrogate a similar complex in the β-cell, where Isl1 appears to be the principal LIM-HD TF rather than, for example, Lhx1 [55]. Considering the protective role of SSBP3, we hypothesized that *SSBP3* loss would yield a more severe phenotype than individual *Ldb1* and *Isl1* knockouts. Surprisingly, *Pax6-Cre* driven SSBP3 knockouts exhibited a slightly delayed hyperglycemic phenotype compared to Ldb1 loss using the same Cre transgene (P10 hyperglycemia in *Ldb1*$^{\Delta Islet}$ [19], P21 in *SSBP3*$^{\Delta Islet}$). While understanding the potential for differential Cre recombination efficiency in these models, there remains the strong possibility for (at least) partial compensation by other SSBP co-regulator family members (e.g., SSBP2 or SSBP4). Our prior study found that *SSBP2* and *SSBP4* are expressed in Min6 β-cell lines, albeit at lower levels than *SSBP3* [21]. These regulators are also expressed in primary mouse and human islet cells, as demonstrated by single-cell and transcriptomic atlases [56–58]. Future studies may further assess their contributions to LIM-containing transcriptional complexes in the β-cell and islet.

Our RNA-Seq analysis highlighted shared DEG signatures between *Isl1*, *Ldb1*, and *SSBP3* adult β-cell knockouts, including *MafA*, *Lmo1*, and GSIS genes (*Pcsk1*, *G6pc2*; Figure 7G). These data provide valuable insight into the targets of β-cell Isl1::Ldb1::SSBP3 complexes, but we also appreciate that the gene targets do not completely overlap between models, perhaps due to activity of other LIM-transcriptional complex components. Combinatorial hexameric Ldb1-mediated complexes employing multiple LIM-HD TFs have been reported in other contexts, including in developing spinal cord neurons (termed the LIM Code [59]). In the β-cell, a similar "code" could exist with Isl1 and other LIM-HD TFs, such as Lhx1. In addition to LIM-HD containing complexes featuring (for example) Isl1, SSBPs also participate in Ldb1-mediated complexes with GATA- and basic helix-loop-helix (bHLH)-class TFs via LIM-only adapter proteins (i.e., Lmo1-4), as shown during erythropoiesis [60–62]. Lmo1, 2, and 4 are expressed in developing and adult islets [19] and may function within these Ldb1::GATA::bHLH transcriptional complexes, also mediated by SSBPs. Perhaps Isl1-independent SSBP3 activity employs GATA4, GATA6 and/or NeuroD1 TFs, all known regulators of pancreatic development [63–66]. Future studies may define whether these complexes have relevance to β- or α-cells.

Limitations of our current study include that, considering a role of SSBP3 in the maintenance of LIM complexes, we did not test protein levels of Isl1 or Ldb1 *in vivo*, which should be examined in future experiments. We also acknowledge that the published *Isl1*- and *Ldb1*-depletion model transcriptomes [16] compared in Figure 7 were conducted using YFP-sorted β-cells while our *SSBP3* knockout RNA was isolated from whole-islets. This may contribute to gene expression differences, but perhaps less so in β-cell specific DEGs. Our focus on β-cell genes allowed us to determine shared targets that were supported by the observed glucose homeostasis and GSIS phenotypes.

The SSBP3 roles detailed in our present study provide many avenues for future efforts. Lineage tracing experiments will help answer the question of potential trans-differentiation in the absence of SSBP3, and thus more specifically define to what extent SSBP3-deficient islet cells adopt other islet or non-islet cell fates. Regarding the LIM transcriptional complexes mentioned above, we also aim to determine other members of these complexes in future studies. The mRNA encoding the LIM-only co-regulator, Lmo1, was decreased across all three models (Figure 7G), suggesting perhaps this is an additional LIM factor with roles in the islet. Another LIM-HD TF, Lmx1b, was implicated in human endocrine progenitor fate *in vitro* [67] and may also be a component of islet SSBP3-mediated complexes, though its levels were not found to be altered in our transcriptome analysis. The increased glucagon^{+} cells, not observed in *Isl1* or *Ldb1* knockouts, also suggests a unique role for SSBP3 in α-cells that will be addressed. Overall, this study establishes SSBP3 co-regulator importance for the development and maintenance of the pancreatic islet, further defining LIM transcriptional complexes in the pancreas. This not only provides new insight into how islet and β-cell function are regulated *in vivo*, but perhaps identifies SSBP3 as a novel islet regulator to be examined in future *in vitro* cell-based therapies.

DECLARATION OF COMPETING INTEREST

The authors declare that they have no known competing financial interests or personal relationships that could have appeared to influence the work reported in this paper.

DATA AVAILABILITY

Gene expression data are publicly available in GEO upon article publication.

ACKNOWLEDGMENTS

This work was supported by NIH/National Institute of Diabetes and Digestive and Kidney Diseases (NIDDK) R01 awards (DK111483 and DK128132 to CSH), F31

DK120217 (to ET), F31 DK121414 (to JDK), F31 DK111181 (to MMB), an NIH/National Institute of General Medical Sciences (NIGMS) Translational and Molecular Sciences T32 training grant (T32 GM109780 to JDK), and NIH/NIGMS Cell, Molecular, and Developmental Biology T32 training grant (T32 GM008111 to ET, MMB).
The monoclonal antibodies against Nkx2.2 (developed by Drs. TM Jessell and S Brenner-Morton) and Nkx6.1 (developed by Dr. OD Madsen) were obtained from the Developmental Studies Hybridoma Bank, created by the NICHD of the NIH and maintained at The University of Iowa, Department of Biology, Iowa City, IA 52242. Schematics of our models were generated using BioRender.com [68]. We thank Dr. Lara Ianov (UAB) and Shaurita Hutchins (UAB) for guidance with transcriptomic analyses. We also thank Dr. Ruth Ashery-Padan (Tel Aviv University) for generously sharing the *Pax6-Cre* mouse line.

APPENDIX A. SUPPLEMENTARY DATA

Supplementary data to this article can be found online at https://doi.org/10.1016/j.molmet.2023.101785.

REFERENCES

[1] C.f.D.C.a. Prevention, National Diabetes Statistics Report. 2020.
[2] Bourgeois S, Sawatani T, Van Mulders A, De Leu N, Heremans Y, Heimberg H, et al. Towards a functional cure for diabetes using stem cell-derived beta cells: are we there yet? Cells 2021;10.
[3] Wortham M, Sander M. Transcriptional mechanisms of pancreatic beta-cell maturation and functional adaptation. Trends Endocrinol Metab 2021;32:474–87.
[4] Steiner DJ, Kim A, Miller K, Hara M. Pancreatic islet plasticity: interspecies comparison of islet architecture and composition. Islets 2010;2:135–45.
[5] Campbell JE, Newgard CB. Mechanisms controlling pancreatic islet cell function in insulin secretion. Nat Rev Mol Cell Biol 2021;22:142–58.
[6] Wendt A, Eliasson L. Pancreatic alpha-cells - the unsung heroes in islet function. Semin Cell Dev Biol 2020;103:41–50.
[7] Rorsman P, Huising MO. The somatostatin-secreting pancreatic delta-cell in health and disease. Nat Rev Endocrinol 2018;14:404–14.
[8] Wierup N, Sundler F, Heller RS. The islet ghrelin cell. J Mol Endocrinol 2014;52:R35–49.
[9] Ediger BN, Du A, Liu J, Hunter CS, Walp ER, Schug J, et al. Islet-1 is essential for pancreatic beta-cell function. Diabetes 2014;63:4206–17.
[10] Du A, Hunter CS, Murray J, Noble D, Cai CL, Evans SM, et al. Islet-1 is required for the maturation, proliferation, and survival of the endocrine pancreas. Diabetes 2009;58:2059–69.
[11] Ahlgren U, Pfaff SL, Jessell TM, Edlund T, Edlund H. Independent requirement for ISL1 in formation of pancreatic mesenchyme and islet cells. Nature 1997;385:257–60.
[12] Cai CL, Liang X, Shi Y, Chu PH, Pfaff SL, Chen J, et al. Isl1 identifies a cardiac progenitor population that proliferates prior to differentiation and contributes a majority of cells to the heart. Dev Cell 2003;5:877–89.
[13] Pfaff SL, Mendelsohn M, Stewart CL, Edlund T, Jessell TM. Requirement for LIM homeobox gene Isl1 in motor neuron generation reveals a motor neuron-dependent step in interneuron differentiation. Cell 1996;84:309–20.
[14] Nishimura W, Iwasa H, Tumurkhuu M. Role of the transcription factor MAFA in the maintenance of pancreatic beta-cells. Int J Mol Sci 2022;23.
[15] Liu J, Hunter CS, Du A, Ediger B, Walp E, Murray J, et al. Islet-1 regulates Arx transcription during pancreatic islet alpha-cell development. J Biol Chem 2011;286:15352–60.
[16] Ediger BN, Lim HW, Juliana C, Groff DN, Williams LT, Dominguez G, et al. LIM domain-binding 1 maintains the terminally differentiated state of pancreatic beta cells. J Clin Invest 2017;127:215–29.
[17] Yasuoka Y, Taira M. LIM homeodomain proteins and associated partners: then and now. Curr Top Dev Biol 2021;145:113–66.
[18] Matthews JM, Visvader JE. LIM-domain-binding protein 1: a multifunctional cofactor that interacts with diverse proteins. EMBO Rep 2003;4:1132–7.
[19] Hunter CS, Dixit S, Cohen T, Ediger B, Wilcox C, Ferreira M, et al. Islet alpha-, beta-, and delta-cell development is controlled by the Ldb1 coregulator, acting primarily with the islet-1 transcription factor. Diabetes 2013;62:875–86.
[20] Toren E, Liu Y, Bethea M, Wade A, Hunter CS. The Ldb1 transcriptional co-regulator is required for establishment and maintenance of the pancreatic endocrine lineage. FASEB J 2022;36:e22460.
[21] Galloway JR, Bethea M, Liu Y, Underwood R, Mobley JA, Hunter CS. SSBP3 interacts with islet-1 and Ldb1 to impact pancreatic beta-cell target genes. Mol Endocrinol 2015;29:1774–86.
[22] Chen L, Segal D, Hukriede NA, Podtelejnikov AV, Bayarsaihan D, Kennison JA, et al. Ssdp proteins interact with the LIM-domain-binding protein Ldb1 to regulate development. Proc Natl Acad Sci U S A 2002;99:14320–5.
[23] Ostendorff HP, Peirano RI, Peters MA, Schluter A, Bossenz M, Scheffner M, et al. Ubiquitination-dependent cofactor exchange on LIM homeodomain transcription factors. Nature 2002;416:99–103.
[24] Bach I, Rodriguez-Esteban C, Carriere C, Bhushan A, Krones A, Rose DW, et al. RLIM inhibits functional activity of LIM homeodomain transcription factors via recruitment of the histone deacetylase complex. Nat Genet 1999;22:394–9.
[25] Enkhmandakh B, Makeyev AV, Bayarsaihan D. The role of the proline-rich domain of Ssdp1 in the modular architecture of the vertebrate head organizer. Proc Natl Acad Sci U S A 2006;103:11631–6.
[26] Hingorani SR, Petricoin EF, Maitra A, Rajapakse V, King C, Jacobetz MA, et al. Preinvasive and invasive ductal pancreatic cancer and its early detection in the mouse. Cancer Cell 2003;4:437–50.
[27] Ashery-Padan R, Marquardt T, Zhou X, Gruss P. Pax6 activity in the lens primordium is required for lens formation and for correct placement of a single retina in the eye. Genes Dev 2000;14:2701–11.
[28] Wicksteed B, Brissova M, Yan W, Opland DM, Plank JL, Reinert RB, et al. Conditional gene targeting in mouse pancreatic beta-cells: analysis of ectopic Cre transgene expression in the brain. Diabetes 2010;59:3090–8.
[29] Loyd C, Liu Y, Kim T, Holleman C, Galloway J, Bethea M, et al. LDB1 regulates energy homeostasis during diet-induced obesity. Endocrinology 2017;158:1289–97.
[30] Rabaglia ME, Gray-Keller MP, Frey BL, Shortreed MR, Smith LM, Attie AD. Alpha-Ketoisocaproate-induced hypersecretion of insulin by islets from diabetes-susceptible mice. Am J Physiol Endocrinol Metab 2005;289:E218–24.
[31] Lu B, Chen J, Xu G, Grayson TB, Jing G, Jo S, et al. Alpha cell thioredoxin-interacting protein deletion improves diabetes-associated hyperglycemia and hyperglucagonemia. Endocrinology 2022;163.
[32] Andrews S. FastQC: a quality control tool for high throughput sequence data [Online]. Babraham Bioinformatics; 2010.
[33] Krueger F. Trim Galore: a wrapper tool around Cutadapt and FastQC to consistently apply quality and adapter trimming to FastQ files. Babraham Bioinformatics; 2015.
[34] Dobin A, Davis CA, Schlesinger F, Drenkow J, Zaleski C, Jha S, et al. STAR: ultrafast universal RNA-seq aligner. Bioinformatics 2013;29:15–21.
[35] Liao Y, Smyth GK, Shi W. The R package Rsubread is easier, faster, cheaper and better for alignment and quantification of RNA sequencing reads. Nucleic Acids Res 2019;47:e47.
[36] Love MI, Huber W, Anders S. Moderated estimation of fold change and dispersion for RNA-seq data with DESeq2. Genome Biol 2014;15:550.
[37] Kolde R. pheatmap: Pretty Heatmaps. 2019.
[38] Yu G, Wang LG, Han Y, He QY. clusterProfiler: an R package for comparing biological themes among gene clusters. OMICS 2012;16:284–7.

[39] Wu T, Hu E, Xu S, Chen M, Guo P, Dai Z, et al. clusterProfiler 4.0: a universal enrichment tool for interpreting omics data. Innovation (Camb) 2021;2:100141.
[40] Wickham H. ggplot2: elegant graphics for data analysis. 2016.
[41] Magnuson MA, Osipovich AB. Pancreas-specific Cre driver lines and considerations for their prudent use. Cell Metab 2013;18:9–20.
[42] Hill JT, Chao CS, Anderson KR, Kaufman F, Johnson CW, Sussel L. Nkx2.2 activates the ghrelin promoter in pancreatic islet cells. Mol Endocrinol 2010;24:381–90.
[43] Prado CL, Pugh-Bernard AE, Elghazi L, Sosa-Pineda B, Sussel L. Ghrelin cells replace insulin-producing beta cells in two mouse models of pancreas development. Proc Natl Acad Sci U S A 2004;101:2924–9.
[44] Dahan T, Ziv O, Horwitz E, Zemmour H, Lavi J, Swisa A, et al. Pancreatic beta-cells express the fetal islet hormone gastrin in rodent and human diabetes. Diabetes 2017;66:426–36.
[45] Mauvais-Jarvis F. Sex differences in metabolic homeostasis, diabetes, and obesity. Biol Sex Differ 2015;6:14.
[46] Alemany M. Estrogens and the regulation of glucose metabolism. World J Diabetes 2021;12:1622–54.
[47] van der Meulen T, Mawla AM, DiGruccio MR, Adams MW, Nies V, Dolleman S, et al. Virgin beta cells persist throughout life at a neogenic niche within pancreatic islets. Cell Metab 2017;25:911–926 e6.
[48] Yu J, Ma J, Li Y, Zhou Y, Luo L, Yang Y. Pax4-Ghrelin mediates the conversion of pancreatic epsilon-cells to beta-cells after extreme beta-cell loss in zebrafish. Development 2023;150.
[49] Sharon N, Chawla R, Mueller J, Vanderhooft J, Whitehorn LJ, Rosenthal B, et al. A peninsular structure coordinates asynchronous differentiation with morphogenesis to generate pancreatic islets. Cell 2019;176:790–804 e13.
[50] Artner I, Hang Y, Mazur M, Yamamoto T, Guo M, Lindner J, et al. MafA and MafB regulate genes critical to beta-cells in a unique temporal manner. Diabetes 2010;59:2530–9.
[51] Zhang C, Moriguchi T, Kajihara M, Esaki R, Harada A, Shimohata H, et al. MafA is a key regulator of glucose-stimulated insulin secretion. Mol Cell Biol 2005;25:4969–76.
[52] Nishioka N, Nagano S, Nakayama R, Kiyonari H, Ijiri T, Taniguchi K, et al. Ssdp1 regulates head morphogenesis of mouse embryos by activating the Lim1-Ldb1 complex. Development 2005;132:2535–46.
[53] Mukhopadhyay M, Teufel A, Yamashita T, Agulnick AD, Chen L, Downs KM, et al. Functional ablation of the mouse Ldb1 gene results in severe patterning defects during gastrulation. Development 2003;130:495–505.
[54] Shawlot W, Behringer RR. Requirement for Lim1 in head-organizer function. Nature 1995;374:425–30.
[55] Bethea M, Liu Y, Wade AK, Mullen R, Gupta R, Gelfanov V, et al. The islet-expressed Lhx1 transcription factor interacts with Islet-1 and contributes to glucose homeostasis. Am J Physiol Endocrinol Metab 2019;316:E397–409.
[56] Krentz NAJ, Lee MYY, Xu EE, Sproul SLJ, Maslova A, Sasaki S, et al. Single-cell transcriptome profiling of mouse and hESC-derived pancreatic progenitors. Stem Cell Rep 2018;11:1551–64.
[57] Segerstolpe A, Palasantza A, Eliasson P, Andersson EM, Andreasson AC, Sun X, et al. Single-cell transcriptome profiling of human pancreatic islets in health and type 2 diabetes. Cell Metab 2016;24:593–607.
[58] DiGruccio MR, Mawla AM, Donaldson CJ, Noguchi GM, Vaughan J, Cowing-Zitron C, et al. Comprehensive alpha, beta and delta cell transcriptomes reveal that ghrelin selectively activates delta cells and promotes somatostatin release from pancreatic islets. Mol Metab 2016;5:449–58.
[59] Thor S, Andersson SG, Tomlinson A, Thomas JB. A LIM-homeodomain combinatorial code for motor-neuron pathway selection. Nature 1999;397:76–80.
[60] Xu Z, Meng X, Cai Y, Liang H, Nagarajan L, Brandt SJ. Single-stranded DNA-binding proteins regulate the abundance of LIM domain and LIM domain-binding proteins. Genes Dev 2007;21:942–55.
[61] Love PE, Warzecha C, Li L. Ldb1 complexes: the new master regulators of erythroid gene transcription. Trends Genet 2014;30:1–9.
[62] Matthews JM, Bhati M, Craig VJ, Deane JE, Jeffries C, Lee C, et al. Competition between LIM-binding domains. Biochem Soc Trans 2008;36:1393–7.
[63] Carrasco M, Delgado I, Soria B, Martin F, Rojas A. GATA4 and GATA6 control mouse pancreas organogenesis. J Clin Invest 2012;122:3504–15.
[64] Xuan S, Borok MJ, Decker KJ, Battle MA, Duncan SA, Hale MA, et al. Pancreas-specific deletion of mouse Gata4 and Gata6 causes pancreatic agenesis. J Clin Invest 2012;122:3516–28.
[65] Naya FJ, Huang HP, Qiu Y, Mutoh H, DeMayo FJ, Leiter AB, et al. Diabetes, defective pancreatic morphogenesis, and abnormal enteroendocrine differentiation in BETA2/neuroD-deficient mice. Genes Dev 1997;11:2323–34.
[66] Mastracci TL, Anderson KR, Papizan JB, Sussel L. Regulation of Neurod1 contributes to the lineage potential of Neurogenin3+ endocrine precursor cells in the pancreas. PLoS Genet 2013;9:e1003278.
[67] Alvarez-Dominguez JR, Donaghey J, Rasouli N, Kenty JHR, Helman A, Charlton J, et al. Circadian entrainment triggers maturation of human in vitro islets. Cell Stem Cell 2020;26:108–122 e10.
[68] Created with. 2023. BioRender.com.

